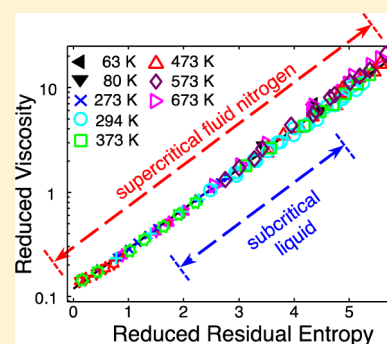


Viscosity of Fluid Nitrogen to Pressures of 10 GPa

Evan H. Abramson*

Department of Earth and Space Sciences, University of Washington, Seattle, Washington 98195-1310, United States

ABSTRACT: Shear viscosities of supercritical nitrogen have been measured in the high-pressure diamond-anvil cell, to 673 K and pressures in excess of 10 GPa, using a rolling-sphere technique. The entire set of data, along with lower pressure data from the literature, can be fit to a two-parameter expression in reduced viscosity and reduced residual entropy. The fit spans densities from the dilute gas to 5x the critical density, and two orders magnitude in temperature and in viscosity, with a maximum deviation of 20%. Reduced viscosities scale as ρ^4/T and comport with the theory of state “isomorphs” for “Roskilde-simple” systems. The new data allow direct comparison with results of molecular dynamic simulations at high densities.



INTRODUCTION

Shear viscosities of supercritical nitrogen have previously been measured to 573 K and 7 GPa.¹ We report here additional measurements, up to temperatures of 673 K and pressures in excess of 10 GPa. Viscosities of high-density nitrogen are relevant to the studies of planetary interiors, explosives, and high-pressure chemical synthesis; the inferred short-range, intermolecular forces may usefully inform calculations of, e.g., high-energy molecular collisions. As well, fluid nitrogen and its viscosities provide an interesting example of the phenomenon of “isomorphs”, “Roskilde-simple” systems, and the relation between viscosity and residual entropy.

EXPERIMENTAL METHODS

Viscosity is determined from the measured speed of a platinum sphere rolling in a high-pressure, diamond-anvil cell inclined with respect to the vertical. For a given pressure and temperature speed is recorded at several angles of inclination. A plot of speed against the sine of the angle gives a straight line, with a slope inversely proportional to viscosity. Additional details of the technique are described in refs 1–4. Pressures, measured by the fluorescence of samarium-doped SrB_4O_7 ,⁵ are precise to 0.02 GPa and temperatures of the cell (enclosed in an oven) are measured with Chromel–Alumel thermocouples to 1 K. Obtained viscosities demonstrate a root-mean-square (rms) scatter rising from ~3% at 294 K to 5% at 673 K.

RESULTS

Data from this and the preceding study¹ are plotted as functions of pressure along five isotherms in Figure 1.

The isotherms can not be reasonably described as exponential functions of pressure, as is sometimes assumed, but are instead well fit by

$$\ln(\eta) = \ln\left[\frac{\eta_{\text{dilute}}\rho_0}{(B-1)\rho + \rho_0}\right] + B\left[\frac{\rho}{\rho_0 - \rho}\right] \quad (1)$$

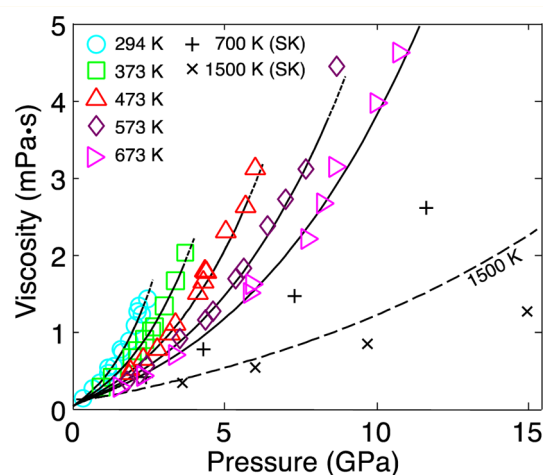


Figure 1. Measured viscosities are plotted on isotherms against pressure, along with results from molecular dynamic simulations (SK).⁶ Solid lines are from eq 1, extended by short dashes in the metastable region above the melting points; long dashes show a 1500 K isotherm as predicted by eq 3

where ρ is the density, η_{dilute} is the (density-independent) viscosity of the dilute gas⁷ at the appropriate temperature, and B and ρ_0 are constants for each isotherm. A simultaneous fit to all data in Figure 1 yields $B = 6.75 + 1.93 \times 10^{-2}T$ and ρ_0 (g/cm^3) = $1.91 + 7.57 \times 10^{-3}T$ with an overall rms deviation of 4.7%. All calculated thermodynamic parameters are taken from an equation-of-state (EOS) written⁸ as an expansion of the Helmholtz energy in density and inverse temperature; the EOS was developed so as to obtain reasonable results in extrapolation to regions of pressure and temperature for which little or no thermodynamic data exist (above 2 GPa only

Received: August 6, 2014

Revised: September 10, 2014

Published: September 12, 2014

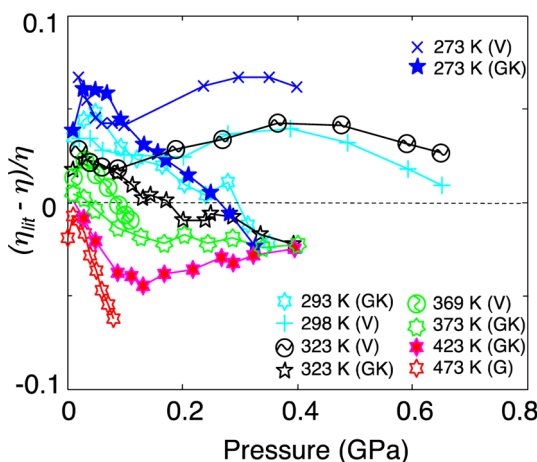


Figure 2. Fractional deviations between lower pressure data from the literature [(V);⁹ (GK);¹⁰ (G)¹¹], η_{lit} and the predictions of eq 1 are plotted against pressure along isotherms. Absolute viscosities range between 0.02 and 0.2 mPa·s. Line segments are guides to the eye.

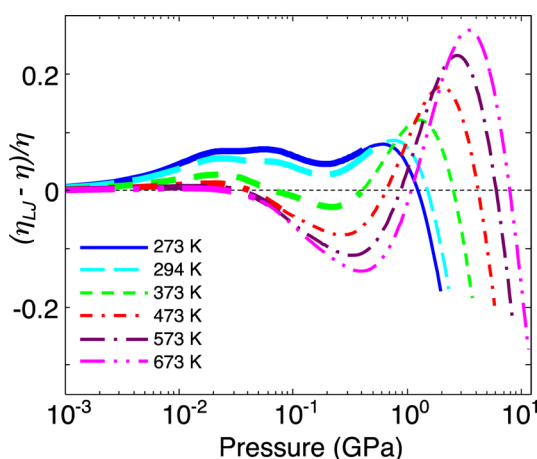


Figure 3. Fractional deviations between the formulation of Lemmon and Jacobsen,⁷ η_{LJ} , and the predictions of eq 1 are plotted against pressure. Thicker sections of line indicate regions in which measured viscosities were available to inform the formulation.

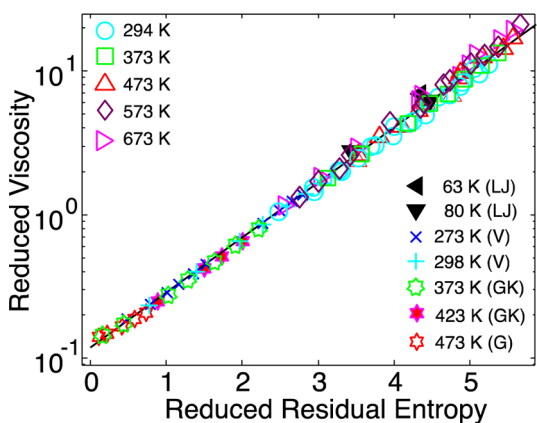


Figure 4. Reduced viscosities are plotted against reduced residual entropies for both current data and lower pressure data from the literature [LJ;⁷ V;⁹ GK;¹⁰ G¹¹]. Deviations from the straight line are less than 20%.

a few shock-derived data are available). Equation 1 gives a good match to lower pressure viscosities^{9–11} not included in the fit

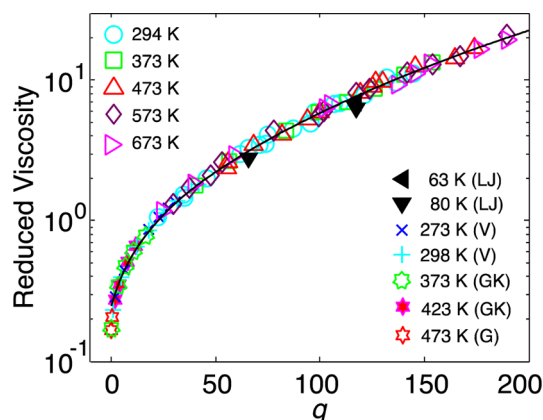


Figure 5. Reduced viscosities are plotted against $q = (\rho/\rho_{crit})^4 / (T/T_{crit})$ for current and literature [LJ;⁷ V;⁹ GK;¹⁰ G¹¹] data. The curve is given by eqs 3, with constants as in the text.

(Figure 2), and so may be useful for interpolation into the range intermediate between the available low- and high-pressure data; it is not expected to yield reasonable extrapolations to higher density. As in the fluids carbon dioxide,¹² argon¹³ and methane,¹⁴ viscosities are systematically underestimated in the cooler liquid at lower pressures (here, below ~ 0.1 GPa) where attractive forces may be presumed to be more significant.

The comprehensive Lemmon–Jacobsen⁷ formulation of nitrogen's viscosities is based primarily on data taken below 0.1 GPa, with a few sets extending up to 0.6 GPa (as represented in Figure 2). In order to examine the accuracy of eq 1 at lower pressures, and also that of the formulation when extrapolated to higher pressures, fractional differences between the two are displayed in Figure 3.

Regions in which the formulation was supported by existing data are shown in the figure as thicker lines; those data demonstrated a scatter of $\pm 5\%$ at pressures either in excess of 0.1 GPa or outside the temperature interval of 270 to 300 K (uncertainties for the dilute gas are given as 0.5% at all temperatures). Deviations should then be seen, below roughly 0.1 GPa, as an indication of the deficiencies of eq 1, and at higher pressures of errors produced by extrapolation of the Lemmon–Jacobsen formulation. Note that between 0.1 and 1 GPa, for temperatures where data exist, eq 1 provides an accurate interpolation between the current, higher pressure data and the dilute gas values. The negative deviations of the formulation in the same pressure range but at higher temperatures, where eq 1 is similarly supported by data but the formulation is not, might then be presumed due to errors in the latter.

For small molecules the relation between a reduced viscosity, η_{red} , and reduced residual entropy, s , is also usefully considered. The quantities are defined here as

$$\eta_{red} = \eta \rho_{melt}^{-2/3} (mkT)^{-1/2} \text{ and } s = -(S - S_{ideal})/Nk \quad (2)$$

where ρ_{melt} is the particle density of the fluid at its melting point¹⁵ (at the relevant temperature), m is the particle mass, k Boltzmann's constant, and S is the entropy, while S_{ideal} is the entropy the fluid would have if it were an ideal gas at the same density and temperature. Note that the definition of η_{red} given above differs from the usual in that ρ_{melt} is substituted for ρ in order to avoid a divergence at low pressures (values of ρ_{melt} for the 294, 373, 473 573 and 673 K isotherms are taken as 1.33,

Table 1. Measured Pressures, Temperatures, and Viscosities; Calculated Densities and Reduced Residual Entropies

P (GPa)	T (K)	η (mPa·s)	ρ^a (g/cm ³)	s^a	P (GPa)	T (K)	η (mPa·s)	ρ^a (g/cm ³)	s^a
0.34	294.5	0.139	0.843	2.48	3.03	372.2	1.293	1.376	4.93
0.52	294.2	0.199	0.940	2.94	3.39	372.2	1.625	1.413	5.16
0.53	294.5	0.191	0.943	2.95	3.73	371.3	1.941	1.446	5.36
0.69	294.5	0.265	1.004	3.26	1.88	472.7	0.434	1.189	3.51
0.70	294.3	0.254	1.008	3.28	1.92	474.3	0.467	1.195	3.53
0.71	293.5	0.254	1.012	3.31	2.33	474.6	0.619	1.254	3.81
0.85	294.5	0.309	1.055	3.53	2.80	474.3	0.772	1.313	4.09
0.90	294.2	0.338	1.069	3.61	3.21	474.6	0.940	1.358	4.31
0.96	294.0	0.388	1.085	3.69	3.40	473.1	1.045	1.378	4.42
1.00	294.0	0.378	1.095	3.75	4.11	474.4	1.454	1.443	4.76
1.03 ^b	294.7	0.425	1.102	3.79	4.30	474.2	1.670	1.459	4.85
1.12	293.5	0.445	1.125	3.92	4.35	473.5	1.718	1.463	4.88
1.18	295.3	0.470	1.137	3.98	4.40	468.9	1.710	1.469	4.93
1.19	294.3	0.536	1.140	4.00	5.03	474.8	2.238	1.515	5.16
1.35	294.3	0.555	1.173	4.20	5.70	474.3	2.685	1.563	5.44
1.40	294.5	0.586	1.183	4.25	6.03	474.5	3.040	1.584	5.56
1.56	296.0	0.654	1.212	4.41	1.42 ^b	577.8	0.279	1.069	2.76
1.57	293.5	0.693	1.215	4.45	1.73	570.7	0.362	1.131	3.00
1.58	294.2	0.750	1.216	4.45	2.21 ^b	578.2	0.446	1.204	3.28
1.63	294.0	0.725	1.225	4.50	2.40	570.7	0.524	1.233	3.41
1.72 ^b	294.8	0.843	1.239	4.59	3.50	571.3	0.881	1.358	3.95
1.75	294.7	0.884	1.244	4.62	4.35	573.5	1.129	1.445	4.35
1.79	293.5	0.886	1.251	4.67	4.58	572.7	1.228	1.452	4.39
1.80	294.2	0.871	1.253	4.68	5.30	573.3	1.649	1.506	4.65
1.86	294.7	0.883	1.262	4.73	5.62 ^b	577.0	1.829	1.527	4.74
2.02	294.8	1.036	1.286	4.87	6.39	573.2	2.301	1.578	5.01
2.04	294.2	1.081	1.289	4.90	6.95	573.1	2.636	1.611	5.19
2.11	294.7	1.180	1.298	4.96	7.62 ^b	576.8	3.125	1.648	5.37
2.15	294.5	1.235	1.304	4.99	8.63 ^b	576.3	4.436	1.699	5.66
2.21	294.3	1.306	1.312	5.05	1.53 ^b	676.8	0.279	1.061	2.55
2.29	294.5	1.259	1.323	5.12	2.32 ^b	672.8	0.435	1.193	3.02
2.45	294.7	1.468	1.343	5.25	3.41 ^b	674.8	0.702	1.321	3.50
0.93	372.5	0.266	1.034	3.12	5.81 ^b	676.1	1.498	1.516	4.31
1.31	372.5	0.393	1.126	3.57	5.94 ^b	675.0	1.615	1.524	4.35
1.97	371.8	0.669	1.242	4.18	7.71 ^b	673.3	2.201	1.629	4.84
2.16	370.2	0.720	1.271	4.34	8.24 ^b	675.2	2.665	1.656	4.97
2.36	372.2	0.876	1.297	4.47	8.62 ^b	675.3	3.131	1.675	5.06
2.59	369.3	0.982	1.327	4.66	9.97 ^b	675.6	3.974	1.737	5.38
2.70	372.3	1.032	1.339	4.71	10.70 ^b	674.8	4.626	1.768	5.55

^aCalculated from ref 8. ^bNew data, this study.

1.44, 1.58, 1.69, and 1.80 g/cm³, respectively^{8,15}). A semi-logarithmic plot in these variables is given in Figure 4; data from the literature, taken at lower pressures, are also presented. Values for the subcritical liquid at the 63 K liquid–solid–vapor triple point are calculated from the formulation⁷ of Lemmon and Jacobsen, as are those on the 80 K isotherm at the highest (liquid–solid equilibrium) and lowest (liquid–vapor equilibrium) densities.

The plot spans the gas, liquid, and supercritical fluid, densities from those of a dilute gas to a factor of 5.6 larger than the critical density, and temperatures of 63 to 673 K. The line in the figure, given by $\ln(\eta_{red}) = -2.13 + 0.883s$, deviates from the data by at most 20%. At the higher pressures a systematic misfit of the data is obviously correlated with temperature. It is unclear whether this misfit is intrinsic to the relation, or whether it should be ascribed to an inadequacy of the EOS when used in a regime of pressures and temperatures for which only sparse thermodynamic data are available to guide it. A similar plot¹ in which the fluid density, ρ (rather than ρ_{melt}), is

used to reduce viscosity also demonstrates a collapse of the data onto a single curve, albeit not a straight line.

If the fluidity (inverse viscosity) is supposed to be roughly proportional to the number of translational configurations immediately available to a relaxing fluid, itself assumed proportional to the total number of microstates, Ω , such a plot as in Figure 4 should approximate a straight line, which is what is observed. That is, normalizing to an ideal gas at the same temperature and density,

$$\eta_{red}/\eta_{red,ideal} \approx (\Omega_{ideal}/\Omega)^{b \approx 1} \text{ and thus } \ln(\eta_{red}) = \ln(\eta_{red,ideal}) + bs$$

Using Boltzmann's formula for an ideal gas of hard spheres with diameters σ , $\eta_{ideal} = 5(mkT/\pi)^{1/2}/(16\sigma^2)$, and the density at which a hard-sphere fluid freezes,¹⁶ $\rho_{melt} = 0.943/\sigma^3$, we have $\ln(\eta_{red,ideal}) = -1.7$ and, again, b is presumed to have a value of approximately 1.0. These values are encouragingly close to those given above, -2.1 and 0.88 , respectively. Because of

rotational (and vibrational) degrees of freedom it was expected that the value of b should be less than the nominal value of 1.0, as frustrated rotation skews the residual entropies to greater s than would be the case for the loss of purely translational configurations envisaged in the initial presumption. For the systems Ar, N₂, CH₄, and CO₂ the slopes, b , are 0.98, 0.88, 0.86 and 0.70, respectively, showing a convincing progression from spherical monatomic to what might be presumed to be rotationally frustrated systems (intercept values for these three other systems all remain at -2.1).

A plot of reduced viscosity against reduced residual entropy which collapses to a single curve is an example of “isomorphic” behavior in Roskilde-simple^{17–19} systems, although the specific form apparent in Figure 4, a straight line, does not appear to be required. For perfect isomorphs in systems governed by inverse-power law pair potentials, $V(r) \propto r^{-n}$, appropriately reduced dynamic and thermodynamic properties necessarily collapse to a single curve in $\rho^{n/3}/T$; a similar correspondence is approximated in real, Roskilde fluids.

Reduced viscosities of nitrogen have been reported²⁰ to scale as ρ^3/T at lower pressures, a correlation which extends to the current data as seen in Figure 5.

The equations

$$\eta_{\text{red}} = \sum_{i=0}^3 a_i q^i, \quad q = (\rho/\rho_{\text{crit}})^4 / (T/T_{\text{crit}}) \quad (3)$$

with $a_0 = 0.254$, $a_1 = 3.086 \times 10^{-2}$, $a_2 = 9.94 \times 10^{-5}$, $a_3 = 1.521 \times 10^{-6}$ gives a good account of the data at pressures above ~ 0.1 GPa and $\rho > 0.5$ g/cm³ with rms deviation 4.2%, but not at lower pressures (roughly, where the temperature derivative of viscosity changes sign). Use of the actual fluid density to reduce viscosity (theoretically indicated for inverse potentials), rather than the melt density, leads to a somewhat poorer correlation of the extant data, but not sufficiently so as to prefer one over the other.

Strak and Krukowski⁶ used molecular dynamic simulation, coupled with the appropriate Green–Kubo relation, to predict viscosities of nitrogen at 700 and 1500 K, up to a maximum density of 1.8 g/cm³; these predictions are included in Figure 1. The short extension from current, 673 K data indicates that simulations of the 700 K fluid underestimate viscosity by about a factor of 2 at the higher densities. Results of the 1500 K simulation may be compared with values derived from eq 3, using the fitted constants, keeping in mind that the much larger extrapolation both in the equation and in the EOS lead to larger uncertainties. Strak and Krukowski noted that their results for higher densities deviated strongly from the Lemmon–Jacobsen formulation⁷ which latter was fit to previously available (<0.7 GPa) experimental data, and attributed these deviations to a poor extrapolation of the formulation. We see here that the deviations persist in the face of actual data at comparable density and temperature.

CONCLUSION

Viscosities of nitrogen have been measured in the high-pressure diamond-anvil cell between 294 and 673 K. Measured viscosities from this study and the previous¹ are given in Table 1, along with calculated densities and reduced residual entropies. Equations are provided which serve to interpolate both within these data and between these data and the dilute gas, and to extrapolate to higher densities and temperatures. Viscosities are closely correlated with residual entropy and

provide an example of isomorphs within a Roskilde-simple fluid system. Previously published results of molecular dynamic simulations are shown to be inaccurate at high densities.

AUTHOR INFORMATION

Corresponding Author

*(E.H.A.) Telephone: 206-616-4388. Fax: 206-543-0489. E-mail: evan@ess.washington.edu.

Notes

The author declares no competing financial interest.

ACKNOWLEDGMENTS

This work was supported by the Department of Energy, Contract No. DE-NA0001843.

REFERENCES

- (1) Abramson, E. H.; West-Foyle, H. Viscosity of Nitrogen Measured to Pressures of 7 GPa and Temperatures of 573 K. *Phys. Rev. E* **2008**, *77*, 041202–1–5.
- (2) Abramson, E. H. The Shear Viscosity of Supercritical Oxygen at High Pressure. *J. Chem. Phys.* **2005**, *122*, 84501–5.
- (3) Abramson, E. H. Viscosity of Water Measured to Pressures of 6 GPa and Temperatures of 300°C. *Phys. Rev. E* **2007**, *76*, 051203–1–6.
- (4) Abramson, E. H. Rolling Sphere Viscometry in a Diamond Anvil Cell. In *Experimental Thermodynamics, Vol. IX: Advances in Transport Properties of Fluids*; Assael, M. J., Goodwin, A. R. H., Vesovic, V., Wakeham, W. A., Eds.; Royal Society of Chemistry: Cambridge, U.K., 2014; pp 108–113 DOI: 10.1039/9781782625254.
- (5) Abramson, E. H.; Brown, J. M. Equation of State of Water Based on Speeds of Sound Measured in the Diamond-Anvil Cell. *Geochim. Cosmochim. Acta* **2004**, *68*, 1827–35.
- (6) Strak, P.; Krukowski, S. J. Determination of Shear Viscosity of Molecular Nitrogen (N₂): Molecular Dynamic Hard Rotor Methodology and the Results. *Phys. Chem. B* **2011**, *115*, 4359–68.
- (7) Lemmon, E. W.; Jacobsen, R. T. Viscosity and Thermal Conductivity Equations for Nitrogen, Oxygen, Argon, and Air. *Int. J. Thermophys.* **2004**, *25*, 21–69.
- (8) Span, R.; Lemmon, E. W.; Jacobsen, R. T.; Wagner, W.; Yokozeki, A. A Reference Equation of State for the Thermodynamic Properties of Nitrogen for Temperatures from 63.151 to 1000 K and Pressures to 2200 MPa. *J. Phys. Chem. Ref. Data* **2000**, *29*, 1361–1433.
- (9) Vermeesse, J. Mesure du Coefficient de Viscosité de L’Azote a Haute Pression. *Ann. Phys. (Paris)* **1969**, *4*, 245–52.
- (10) Golubev, I. F.; Kurin, V. I. Measuring the Viscosity of Gases at Pressures up to 4000 kgf/cm² and at Different Temperatures. *Therm. Eng. (Transl. of Teploenergetika (Moscow))* **1974**, *21*, 121–5; *Teploenergetika (Moscow)* **1974**, *21*, 83–5.
- (11) Golubev, I. F. *Viscosity of Gases and Gas Mixtures (A Handbook)*; Israel Program for Scientific Translations: Jerusalem, 1970; p 76.
- (12) Abramson, E. H. Viscosity of Carbon Dioxide Measured to a Pressure of 8 GPa and Temperature of 673 K. *Phys. Rev. A* **2009**, *80*, 021201–1–3.
- (13) Abramson, E. H. Viscosity of Argon to 5 GPa and 673 K. *High Pressure Res.* **2011**, *31*, 544–8.
- (14) Abramson, E. H. Viscosity of Methane to 6 GPa and 673 K. *Phys. Rev. E* **2011**, *84*, 062201–1–4.
- (15) Vos, W. L.; Schouten, J. A. Improved Phase Diagram of Nitrogen up to 85 Kbar. *J. Chem. Phys.* **1989**, *91*, 6302–5.
- (16) Hoover, W. G.; Ree, F. H. Melting Transition and Communal Entropy for Hard Spheres. *J. Chem. Phys.* **1968**, *49*, 3609–17.
- (17) Schroder, T. B.; Bailey, N. P.; Pedersen, U. R.; Gnan, N.; Dyre, J. C. Pressure-Energy Correlations in Liquids. III. Statistical Mechanics and Thermodynamics of Liquids with Hidden Scale Invariance. *J. Chem. Phys.* **2009**, *131*, 234503–1–17.
- (18) Gnan, N.; Schroder, T. B.; Pedersen, U. R.; Bailey, N. P.; Dyre, J. C. Pressure-Energy Correlations in Liquids. IV. “Isomorphs” in Liquid Phase Diagrams. *J. Chem. Phys.* **2009**, *131*, 234504–1–18.

- (19) Dyre, J. C. Hidden Scale Invariance in Condensed Matter. *J. Phys. Chem. B* **2014**, *118*, 10007–10024.
- (20) Fragiadakis, D.; Roland, C. M. Connection between Dynamics and Thermodynamics of Liquids on the Melting Line. *Phys. Rev. E* **2011**, *83*, 031504–1–8.